Linear response and the Thomas-Fermi approximation in undoped graphene

L. Brey
Instituto de Ciencia de Materiales de Madrid (CSIC), Cantoblanco 28049, Spain

H. A. Fertig
Department of Physics, Indiana University, Bloomington, Indiana 47405, USA

(Received 28 April 2009; revised manuscript received 17 June 2009; published 8 July 2009)

We analyze the range of validity of Thomas-Fermi theory for describing charge-density modulations induced by external potentials in neutral graphene. We compare exact results obtained from a tight-binding calculation with those of linear-response theory and the Thomas-Fermi approximation. For experimentally interesting ranges of size and density amplitudes (electron densities less than $\sim 10^{11}$ cm^{-2}, and spatial length scales below ~ 20 nm), linear response is significantly more accurate than Thomas-Fermi theory.

DOI: 10.1103/PhysRevB.80.035406 PACS number(s): 81.05.Uw, 71.15.Mb, 73.20.−r

I. INTRODUCTION

The realization of single flakes of grapheme—atomically thin layers of carbon atoms packed in a honeycomb lattice—has made possible the experimental study of two-dimensional (2D) massless Dirac fermions.[1–3] Graphene is a gapless semiconductor in which the conduction and valence bands touch at two points—Dirac points—in the Brillouin zone.[4] Near either of these points the electronic states are described by a massless Dirac equation, with eigenstates that are spinors due to the two-point basis needed to describe the honeycomb lattice.[5] The effective spinors of the wave functions are either parallel or antiparallel to the momentum, so that the states are chiral.

For undoped graphene there is one electron per carbon atom, and the system ideally should be everywhere charge neutral. In practice this is known not to be the case. Recent imaging experiments[6] have demonstrated the existence of electron and hole puddles of densities $\sim 10^{10}$–10^{11} cm^{-2} in the vicinity of the neutrality point. The existence of these charge puddles could be related to the existence of mechanical ripples also observed in graphene sheets,[7–9] which can cause modulation of the electronic charge,[10,11] or to unintentional charged impurities in the substrate,[12–14] which can also generate electron-hole puddles.[15–17] The spatial-correlation length of these puddles is on the order of 10 nm.

Local density inhomogeneities can also be induced in graphene using miniature gates. In this way graphene *p-n* junctions have been experimentally realized.[18–20] Recent advances in the quality of graphene have made possible the fabrication of ballistic circuits with electrically controlled *p-n* junctions.[21,22]

The physical properties of graphene with such electronic inhomogeneities depend strongly on the size and amplitude of charge modulation induced by external potentials. It is therefore important to understand how the ground-state charge in graphene is distributed in their presence. Large inhomogeneous graphene systems have been studied theoretically using the Thomas-Fermi (TF) approximation, which, as we discuss below, treats the kinetic energy in a local-density approximation.[23] Rossi and Das Sarma[15] used a TF approximation with Hartree and exchange effects included to study the ground state of neutral graphene in the presence of charged impurities. A more rigorous quantum-mechanical treatment of the kinetic energy is possible, but its use limits considerably the system sizes which in practice can be studied.[16]

As we will show below, because of the crossing of the chiral electron and hole bands at the Dirac point, the TF approximation does not correctly capture the charge response of neutral graphene to an external potential in many interesting situations. The purpose of this work is to analyze the range of validity of the TF theory near the Dirac point. We use a microscopic tight-binding calculation to compute the response of neutral graphene to electrostatic potentials, and compare these exact results both with linear response and with the TF approximation. We will demonstrate that for experimentally interesting[6] ranges of sizes and amplitudes (electron-densities $\sim 10^{11}$ cm^{-2} and spatial-correlations ~ 20 nm), simple linear-response results match exact results quite well, while results of the TF approach are much poorer. The failure of the TF approximation is related to the nonlocal character of the density response, and we shall see that a kinetic-energy functional that correctly captures the linear response of neutral graphene to external electrostatic perturbations has a highly nonlocal nature.

II. THOMAS-FERMI FUNCTIONAL FOR THE KINETIC ENERGY

A. Formal considerations

Following Hohenberg and Kohn,[24] the total energy of the noninteracting system, E, may be written in terms of a kinetic-energy functional $T[n(\mathbf{r})]$ of the electron-density $n(\mathbf{r})$,

$$E[n(\mathbf{r})] = \int T[n(\mathbf{r})]d\mathbf{r} + \int V(\mathbf{r})n(\mathbf{r})d\mathbf{r}. \quad (1)$$

Here $V(\mathbf{r})$ is the one-body external potential in which the particles move, and the density is defined with respect to the density of electrons in neutral graphene. The effect of electron-electron interactions in a Hartree approximation will be considered below in Sec. III.

The TF theory assumes that the functional $T[n(\mathbf{r})]$ is a local function of the density, and the form of the functional is

chosen such that for a uniform potential V the minimization of Eq. (1) recovers the kinetic energy of a homogeneous system. For the case of Dirac fermions, the Thomas-Fermi kinetic-energy functional is

$$T[n] = \hbar v_F \frac{2\sqrt{\pi}}{3} \mathrm{sgn}[n(\mathbf{r})]|n(\mathbf{r})|^{3/2}, \tag{2}$$

where v_F is the Fermi velocity of the carriers near the Dirac point. The minimization with respect to the density must be carried out subject to the normalization constraint

$$\frac{1}{S}\int n(\mathbf{r})d\mathbf{r} = n_0, \tag{3}$$

where n_0 is the average electron density measured relative to that of undoped graphene, and S is the sample area. Minimizing Eq. (1) yields the relation

$$n^{TF}(\mathbf{r}) = \frac{1}{\hbar^2 v_F^2 \pi} \mathrm{sgn}[\mu_0 - V(\mathbf{r})][\mu_0 - V(\mathbf{r})]^2, \tag{4}$$

where $\mu_0 = \hbar v_F \sqrt{\pi n_0}$ is the Fermi energy of the corresponding homogeneous system. Defining $k_{\max}(\mathbf{r}) = \sqrt{\pi |n^{TF}(\mathbf{r})|}$, we find that the carriers have higher kinetic energy where the potential energy is lower, and vice-versa. Equation (4) can be viewed as the relation between the local maximum momentum $k_{\max}(\mathbf{r})$ and the external potential $V(\mathbf{r})$ obtained from a classical equation of motion.

An interesting and important consistency check of the TF approximation[24] is that the response function of the system should be directly related to the second functional derivative of the energy. For a noninteracting system this takes the form

$$\mathcal{F}\left(\left. \frac{\delta^2 T[n(\mathbf{r})]}{\delta n(\mathbf{r}_1)\delta n(\mathbf{r}_2)} \right|_{n_0} \right) = -\frac{1}{\chi_{\mathrm{Lin}}(q,n_0)}, \tag{5}$$

where $\mathcal{F}$ indicates the Fourier transform, and $\chi_{\mathrm{Lin}}(q,n_0)$ is the wavevector dependent static Lindhard susceptibility of the uniform system at density n_0.

In graphene the Lindhard static susceptibility in the long-wavelength limit has the form[14,25,26]

$$\chi_{\mathrm{Lin}}(q,n_0) = -\frac{2}{\sqrt{\pi}} \frac{|n_0|^{1/2}}{\hbar v_F} \quad \text{for } q < \sqrt{\pi n_0},$$

$$\chi_{\mathrm{Lin}}(q,n_0) = -\frac{q}{4\hbar v_F} \quad \text{for } n_0 = 0. \tag{6}$$

The TF kinetic-energy functional, Eq. (2), correctly recovers the response function for doped graphene in the long-wavelength limit, but it fails to describe the noninteracting compressibility at the neutrality point. In fact, the TF approximation predicts vanishing linear response at the Dirac point. This failure is in agreement with the general assumption of the TF theory that $|\nabla n(\mathbf{r})|/[n(\mathbf{r})k_{\max}(\mathbf{r})] \ll 1$, which cannot be satisfied near charge neutrality. Moreover, as we discuss below, the response in the second of Eq. (6) is inherently nonlocal, suggesting that the TF approximation must break down near charge neutrality.

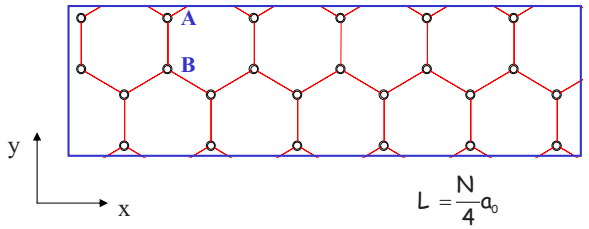

FIG. 1. (Color online) Unit cell used in the calculations. The unit cell contains N atoms and the length of the unit cell is $L = N/4a_0$. The external potential only depends on x and in this geometry atoms A and B with the same x coordinate have the same charge (Refs. 27). a_0 is the lattice parameter of the triangular lattice.

B. Numerical results

In order to quantify the effects of the failure of the TF approximation to correctly describe the linear response of undoped graphene, we numerically compute the electron density of a net neutral graphene system in an external potential, and compare the results with the TF approximation and with linear-response results. We use a simple tight-binding Hamiltonian with nearest-neighbor hopping, of the form

$$H = t\sum_{\langle i,j \rangle} C_i^+ C_j + \sum_i V_i C_i^+ C_i, \tag{7}$$

where C_i annihilates an electron at site $\mathbf{R}_i$ of the graphene lattice, $t = \frac{2}{\sqrt{3}}\frac{v_F}{a_0}$ is the hopping parameter, a_0 is the lattice parameter of the triangular lattice, and V_i represents the external potential at site $\mathbf{R}_i$. We perform the calculations in a unit cell illustrated in Fig. 1, using periodic boundary conditions in both the x and y directions. The external potential and the induced charge depend only on the x coordinate. In the unit cell represented in Fig. 1 atoms on both sublattices experience the same external potential, so there is no out-of-phase response from atoms on different sublattices.[28]

We study the response of the system to the potential

$$V_i = V_0 \cos(GX_i), \tag{8}$$

where X_i is the x component of the position of the carbon atoms, and V_0 is the amplitude of the perturbation. Figure 2 illustrates a typical result, the electron density induced by a potential of amplitude $V_0 = 50$ meV and period $100a_0$. Also plotted are the density as obtained in linear response, $n^{\mathrm{Lin}}(G) = \chi_{\mathrm{Lin}}(G,0)V_0$, and from the TF approximation, Eq. (4). The density induced by this potential is of the same order as the densities of electron and hole puddles observed experimentally. Note that the linear response reproduces the exact result rather faithfully, whereas for this potential the TF approximation underestimates the response. Moreover, the TF approximation displays plateaulike features when passing through zero density, which are an artifact of the approximation;[23] they appear because TF theory grossly underestimates the ability of the system to screen when the local chemical potential is near the Dirac point. The plateaus may be understood more formally by substituting the perturbation Eq. (8) into Eq. (4) and expanding in harmonics, to obtain

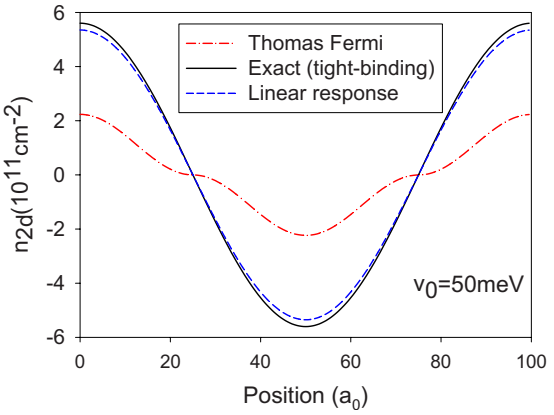

FIG. 2. (Color online) Density profiles obtained with different approximations for perturbation-amplitude $V_0=50$ meV and period $100a_0$. For exact calculations, $t=2.8$ eV and $a_0=2.46$ Å. Solid line is the exact result, dashed line indicates linear-response result, and dash-dotted line is result of Thomas-Fermi approximation.

$$n^{TF}(x) = -\frac{V_0^2\,\mathrm{sgn}(V_0)}{\hbar^2 v_F^2 \pi}\frac{8}{3\pi}\left(\cos Gx + \frac{1}{5}\cos 3Gx + \ldots\right). \tag{9}$$

The large $\cos 3Gx$ harmonic leads to the plateaulike behavior when crossing the Dirac point.

In Fig. 3 we compare the maximum electron density at $x=0$, obtained both from the exact calculation, and in the two different approximation schemes, as a function of V_0, for different periods of the external potential. For small periods and small V_0, the linear-response results follow the exact results rather closely. TF theory by contrast underestimates the response of the system. For small enough V_0 and large G, linear response is able to properly capture the nonlocal nature of screening in this system. For large wavelengths and external potentials nonlinear contributions to the response become important, and may be captured by the TF approximation in any average way [Fig. 3(a)]. From the numerical results we estimate that, in the absence of electron-electron interactions, linear response is more reliable than TF when $n^{\mathrm{Lin}} > n^{TF}$. For large perturbations the exact density response oscillates around the TF result. These oscillations are induced by zero modes created by the external potential in graphene,[29] which cannot be captured by a local approach such as the TF approximation.

For the charge-density modulation amplitudes observed experimentally, $\sim 10^{11}$ cm^{-2}, the length scale for which linear response is more reliable than the TF approximation is larger than the size of the observed electron-hole puddles.[6] Furthermore, from the geometry of the multiple-gated graphene devices in Refs. 21 and 22 we find that the width of the depletion regions in the *p-n* junctions[23] are also smaller than the length scale where linear response is applicable. More generally, our results indicate that *for density modulations up to* 10^{12} cm^{-2} on length scales up to 20 nm, linear-response results are significantly more accurate than those of the TF approximation. This conclusion agrees with results presented in Fig. 2 of Ref. 16, where the authors find results

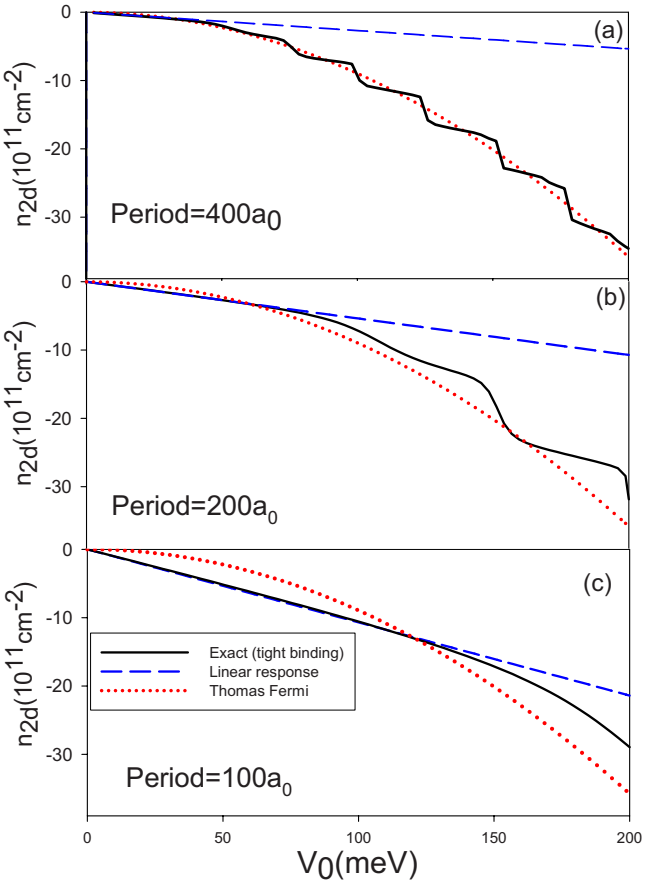

FIG. 3. (Color online) Maximum induced electron density (density at $x=0$) as function of the amplitude of the external potential. The external potential has the form $V(x)=V_0\cos Gx$. (a), (b), And (c) correspond to values $Ga_0=\pi/200$, $Ga_0=\pi/100$, and $Ga_0=\pi/50$, respectively. Continuous lines are the exact results, dashed lines are the linear-response results, and dash-dotted lines are the results obtained in the Thomas-Fermi approximation. In the calculations we use the values $t=2.8$ eV and $a_0=2.46$ Å.

which are consistent at semiquantitative level with a linear screening theory.

III. HARTREE INTERACTION

A. Formulation in terms of linear response

Any modulation of electric charge produces a change in the energy associated with the repulsion between electrons. If one is interested in the long-wavelength static response of the charge density to a potential inducing such a modulation, the most important effects of the electron-electron interaction can be captured by the Hartree energy. This may be written in the form

$$E_H = \frac{1}{2}\frac{e^2}{\varepsilon}\int d\mathbf{r}\int d\mathbf{r}'\frac{n(\mathbf{r})n(\mathbf{r}')}{|\mathbf{r}-\mathbf{r}'|}, \tag{10}$$

where ε is the effective background dielectric constant in the graphene layer. The strength of the Coulomb interaction is given by the dimensionless parameter

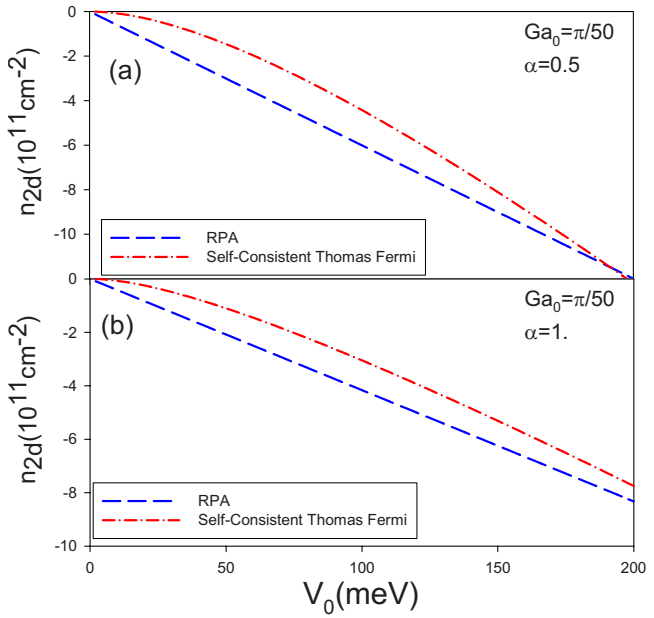

FIG. 4. (Color online) Maximum induced electron density as a function of the amplitude of an external potential of period $100a_0$, in the Hartree approximation. (a) Corresponds to a weak electron-electron interaction, $\alpha=0.5$, and (b) to a stronger one, $\alpha=1$. Dashed lines represent RPA results; dash-dotted lines are results obtained by minimizing an energy functional containing both the TF approximation to the kinetic energy and the Hartree form of the Coulomb interaction.

$$\alpha = \frac{e^2}{\hbar v_F \varepsilon}. \tag{11}$$

In the case of graphene placed on a dielectric substrate with one side exposed to air we set ε equal to the average of the dielectric constant of the air, $\varepsilon_0=1$ and the one of the dielectric, ε_s, so that $\varepsilon=(\varepsilon_0+\varepsilon_s)/2$. In the case of SiO_2, $\varepsilon_s=4$, so that $\varepsilon\approx 2.5$ and $\alpha=0.9$. For substrates with larger ε such as HfO_2 or liquid water, the values of α can be much smaller. We note that in principle one may improve upon the Hartree approximation by including exchange-correlation effects, but for chiral Dirac fermions these appear to be rather small.[16]

Since we will consider perturbations with amplitudes and periods such that the exact noninteracting result coincides nearly perfectly with that of linear response, we expect that the inclusion of the Hartree term leads only to linear screening of the external potential. In this case the induced charge coincides with that obtained in the random-phase approximation (RPA). In reciprocal space this means

$$n^{\text{exact}}(G) \simeq n^{RPA} = \frac{\chi_{\text{Lin}}(G,0)}{1 - v_G \chi_{\text{Lin}}(G,0)} V_0, \tag{12}$$

where $v_q=\frac{2\pi e^2}{\varepsilon q}$ is the two-dimensional Fourier transform of the Coulomb interaction.

In the TF approximation the electron density is obtained by minimizing the kinetic functional, Eq. (1), together with the Hartree energy Eq. (10) with respect to the density. In Fig. 4 we compare the spatial maximum electron density obtained in the RPA to the TF approximation as a function of the amplitude of the external potential. The Hartree interaction screens the external potential, so that the induced charge density decreases with increasing electron-electron interaction-parameter α. As in the noninteracting case we see that the TF approximation underestimates the response at small V_0. For physically relevant values of α, we see that the TF approximation is not quantitatively reliable in describing the response of neutral graphene to external potentials that generate density fluctuations of magnitude 10^{12} cm^{-2} or below, within length scales of about 20 nm.

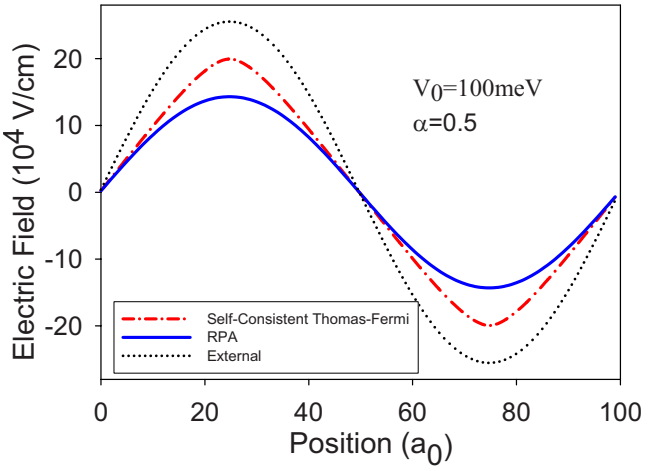

FIG. 5. (Color online) Electric field as a function of position for a periodic external potential of amplitude $V_0=0.1$ eV and period $100a_0$. Coupling constant is taken to be $\alpha=0.5$.

B. Electric fields in a *p-n* junction

Ballistic transport in graphene *p-n* junctions is due to Klein tunneling of the massless electrons. Cheianov and Falko[30] showed that the ballistic resistance per unit width of a graphene *p-n* junction is $R=\frac{\pi}{2}\frac{h}{e^2}\sqrt{\frac{\hbar v_F}{eE}}$, where E is the assumed uniform electric field at the junction. Note the resistance decreases as the electric field at the interface decreases. This electric field depends on the screening properties of graphene near the Dirac point. Zhang and Fogler[23] proposed that the electric field in the depletion region separating the electron and hole regions is enhanced due to the limited screening capacity of Dirac quasiparticles.

In order to study the difference in computed values of F, the electric field in the depletion region, using the TF approximation and linear-response theory, we have calculated the electric field for a cosine-shaped external potential Eq. (8). This potential creates periodic electron and hole regions separated by *p-n* interfaces. In Fig. 5 we plot the electric field as a function of position, as obtained in the TF approximation, and in the RPA (the latter being essentially an exact solution of the Hartree approximation.) For comparison we also plot the applied electric field, $E^{\text{ext}}=-GV_0 \sin Gx$. The results presented are for $\alpha=0.5$. The *p-n* and *n-p* interfaces are located at $x=25a_0$ and $x=75a_0$, respectively. At these points the values of the electric field are maximal. In the linear calculation the electric field F can be calculated analytically, yielding the result $F=V_0G/(1+\pi/2\alpha)$, so that the

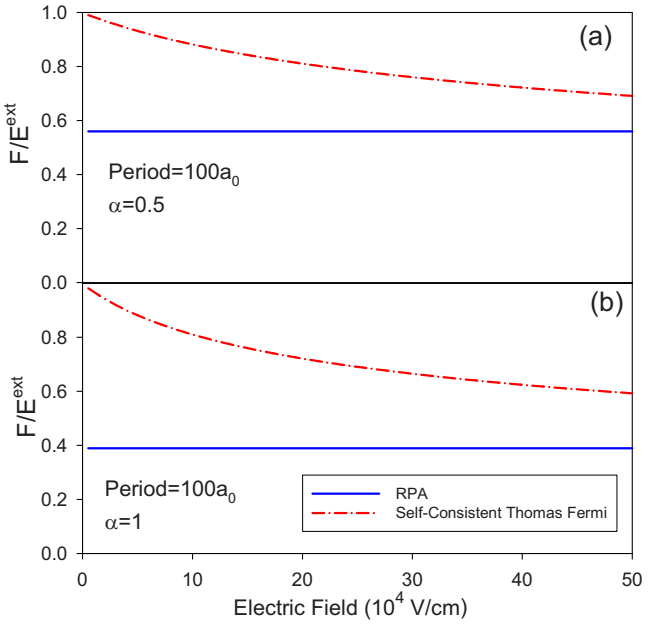

FIG. 6. (Color online) Electric field at the *p-n* junction centers as a function of the external field. (a) corresponds to a weak electron-electron interaction, $\alpha=0.5$ and (b) to a stronger one, $\alpha=1$. Continuous lines corresponds to the RPA results. Dash-dotted lines are the results obtained in the self-consistent Thomas-Fermi approximation.

external electric field is reduced by a factor $(1+\pi/2\alpha)$ by the screening. In the TF approximation a numerical minimization is required to obtain F. In the range of validity of the linear approximation we find that the TF approach predicts much weaker screening of the external field than the RPA.

In Figs. 6(a) and 6(b) we plot the values of the electric field at the *p-n* junctions, normalized to the external field, as a function of the applied electric field, for two different values of α. The screened electric field at the interface obtained from the TF theory is larger than that obtained in the linear-response theory (RPA), as expected from the above results. We see that the TF approximation significantly overestimates the total electric field at the *p-n* junction.

IV. SUMMARY AND OBSERVATIONS

The Thomas-Fermi approximation is relatively inaccurate for describing density modulations for wavevectors that are not too small, and external potentials that are not too large, in undoped graphene. Quantitatively this region of failure of the TF approximation appears to apply to the observed density fluctuations of the electron-hole puddles that appear in the single-electron transistors spectroscopy. It also appears to be problematic for estimating the electric field in a graphene *p-n* junction. The reason for its failure is its inability to capture the intrinsically nonlocal response of neutral graphene. We find that the application of linear-response theory (RPA) in this regime is far more quantitative.

It is interesting to note that one may adopt a nonlocal kinetic-energy functional to produce a correct result for Eq. (5). This takes the form[31]

$$T^{\text{linear}}[n(\mathbf{r})] = \frac{\hbar v_F}{\pi}\int d\mathbf{r}\int d\mathbf{r}'\frac{n(\mathbf{r})n(\mathbf{r}')}{|\mathbf{r}-\mathbf{r}'|}. \tag{13}$$

This kinetic-energy functional is formally the same as the Hartree form of the interaction energy, highlighting the marginal nature of $1/r$ Coulomb interactions in undoped graphene.[4] Its long-range nature strongly suggests the difficulties of a local approximation such as TF that we find.

To improve upon the TF approximation one can formally compute first-order gradient corrections to the density using a WKB approximation applied to Green's function.[32]The result,[33] however, has singular behavior near zero momentum, and moreover depends locally on both the density and its gradient, and so cannot produce corrections where the density is maximum and where TF has significant errors.

Finally we note that Eq. (13) may be used to develop a criterion for which one expects the TF approximation to fail. Using the result of the linear-response density in Eq. (13) gives an estimate for the energy density expected from the nonlocal contribution to the energy. Comparing this to the TF energy-density [Eqs. (2) and (4)], we expect to the latter to be larger if the TF approximation is to be valid. This yields the criterion $V_0/G > \eta\hbar v_F$, where η is a geometric factor of order 1, for which the TF kinetic energy dominates over nonlocal contributions to the energy. Notice this means that, for fixed length-scale $1/G$, the TF approximation will always fail for sufficiently small potential-scales V_0.

ACKNOWLEDGMENTS

We acknowledge useful discussions with F. Guinea, M. Polini, E. Chacón, S. Das Sarma, and A. H. MacDonald. We thank the Aspen Center for Physics for hospitality where this research was initiated, and the KITP at UCSB where it was completed. This work has been financially supported by MEC-Spain (Grant No. MAT2006-03741) and by the National Science Foundation through Grant No. DMR-0704033.

[1] K. S. Novoselov, A. K. Geim, S. V. Mozorov, D. Jiang, Y. Zhang, S. V. Dubonos, I. V. Gregorieva, and A. A. Firsov, Science **306**, 666 (2004).
[2] K. S. Novoselov, D. Jiang, T. Booth, V. Khotkevich, S. M. Morozov, and A. K. Geim, Nature (London) **438**, 197 (2005).
[3] Y. Zhang, Y.-W. Tan, H. L. Stormer, and P. Kim, Nature (London) **438**, 201 (2005).
[4] A. Castro Neto, F. Guinea, N. Peres, K. Novoselov, and A. Geim, Rev. Mod. Phys. **81**, 109 (2009).
[5] T. Ando, J. Phys. Soc. Jpn. **74**, 777 (2005).
[6] J. Martin, N. Akerman, G. Ulbricht, T. Lohmann, J. H. Smet, K. von Klitzing, and A. Yacoby, Nat. Phys. **4**, 144 (2008).

[7] J. C. Meyer, A. K. Geim, M. I. Katsnelson, K. S. Novoselov, T. J. Booth, and S. Roth, Nature (London) **446**, 60 (2007).
[8] E. Stolyarova, K. T. Rim, S. Tyu, J. Maultzsch, P. Kim, L. E. Brus, T. F. Heinz, M. S. Hyberstein, and G. W. Flynn, Proc. Natl. Acad. Sci. U.S.A. **104**, 9209 (2007).
[9] M. Ishigami, J. H. Chen, W. G. Cullen, M. S. Fuhrer, and E. D. Williams, Nano Lett. **7**, 1643 (2007).
[10] L. Brey and J. J. Palacios., Phys. Rev. B **77**, 041403(R) (2008).
[11] F. Guinea, M. I. Katsnelson, and M. A. H. Vozmediano, Phys. Rev. B **77**, 075422 (2008).
[12] E. H. Hwang, S. Adam, and S. Das Sarma, Phys. Rev. Lett. **98**, 186806 (2007).
[13] K. Nomura and A. H. MacDonald, Phys. Rev. Lett. **96**, 256602 (2006).
[14] T. Ando, J. Phys. Soc. Jpn. **75**, 074716 (2006).
[15] E. Rossi and S. Das Sarma, Phys. Rev. Lett. **101**, 166803 (2008).
[16] M. Polini, A. Tomadin, R. Asgari, and A. H. MacDonald, Phys. Rev. B **78**, 115426 (2008).
[17] M. Fogler, arXiv:0810.1755 (unpublished).
[18] B. Huard, J. A. Sulpizio, N. Stander, K. Todd, B. Yang, and D. Goldhaber-Gordon, Phys. Rev. Lett. **98**, 236803 (2007).
[19] B. Ozyilmaz, P. Jarillo-Herrero, D. Efetov, D. A. Abanin, L. S. Levitov, and P. Kim, Phys. Rev. Lett. **99**, 166804 (2007).
[20] J. R. Williams, L. DiCarlo, and C. M. Marcus, Science **317**, 638 (2007).
[21] A. F. Young and P. Kim, Nat. Phys. **5**, 222 (2009).
[22] N. Stander, B. Huard, and D. Goldhaber-Gordon, Phys. Rev. Lett. **102**, 026807 (2009).
[23] L. M. Zhang and M. M. Fogler, Phys. Rev. Lett. **100**, 116804 (2008).
[24] P. Hohenberg and W. Kohn, Phys. Rev. **136**, B864 (1964).
[25] E. H. Hwang and S. Das Sarma, Phys. Rev. B **75**, 205418 (2007).
[26] B. Wunsch, T. Stauber, F. Sols, and F. Guinea, New J. Phys. **8**, 318 (2006).
[27] L. Brey and H. A. Fertig, Phys. Rev. B **73**, 235411 (2006).
[28] L. Brey, H. A. Fertig, and S. Das Sarma, Phys. Rev. B **73**, 195408 (2006).
[29] L. Brey and H. Fertig, arXiv:0904.0540, Phys. Rev. Lett. (to be published).
[30] V. Cheianov and V. Fal'ko, Phys. Rev. B **74**, 041403(R) (2006).
[31] The authors thank A. H. MacDonald for pointing this out.
[32] D. Pfirsch and R. N. Sudan, J. Math. Phys. **32**, 1774 (1991).
[33] H. A. Fertig (unpublished).